Design and behaviour of geosynthetic-reinforced soil walls constructed on yielding foundations

G. D. Skinner[1] and R. K. Rowe[2]

[1]*Assistant Professor, Department of Civil Engineering and GeoEngineering Centre at Queen's-RMC, Queen's University, Kingston, Ontario, K7L 3N6 Canada, Telephone: +1 613 533 3124, Telefax: +1 613 533 2128, E-mail: skinner@civil.queensu.ca*
[2]*Vice-Principal (Research), GeoEngineering Centre at Queen's-RMC, Queen's University, Mackintosh-Corry Hall, F407, Kingston, Ontario, K7L 3N6 Canada, Telephone: +1 613 533 6933, Telefax: +1 613 533 6934, E-mail: rowek@post.queensu.ca*

Received 13 June 2003, revised 9 December 2003, accepted 14 December 2003

ABSTRACT: The short- and long-term behaviour of a 6 m high segmental block-faced geosynthetic-reinforced retaining wall constructed on a rigid base and two 10 m thick clay foundations (one relatively inviscous and one viscoplastic) were numerically investigated to assess the effect of yielding in the foundation deposit on the internal and external stability of the wall. The influence of the rate of loading on the undrained shear strength of the viscoplastic foundation clay deposit is examined. The overall short- and long-term behaviour of the reinforced soil wall, including reinforcement strains and deformations, are discussed and compared with the expected design values. It is shown that the viscoplastic nature of some clayey soils can cause a decrease in the undrained shear strength with time by as much as 20% and increase the reinforcement strains by as much as 45% relative to expected design values.

KEYWORDS: Geosynthetics, Design and behaviour, Numerical analysis, Reinforced retaining walls, Yielding viscoplastic foundation

REFERENCE: Skinner G. D. and Rowe R. K. (2003). Design and behaviour of geosynthetic-reinforced soil walls constructed on yielding foundations. *Geosynthetics International*, **10**, No. 6, 200–214

1. INTRODUCTION

The behaviour of a geosynthetic-reinforced soil wall constructed on a competent (very stiff or rigid) foundation material has been extensively researched—both experimentally and theoretically—in the past, and many current design codes are partially based on this research (Bathurst and Benjamin 1990; Bathurst and Simac 1994; Bathurst *et al.* 1988, 1989; CGS 1992; FHWA 1996; Helwany *et al.* 1999; Ho and Rowe 1993; Karpurapu and Bathurst 1992; Michalowski 1998; NCMA 1996; Porbaha *et al.* 2000; Rowe and Ho 1993, 1996; Wu 1992a,b). However, the same cannot be said for foundation soils that experience plastic yielding due to the loading induced by wall construction (referred to herein as yielding foundations), and there has been very little previous research into the effect of yielding in the foundation on the overall performance of reinforced walls.

It has been widely recognised that one of the main advantages of a geosynthetic-reinforced soil wall constructed on a non-rigid foundation is its ability to withstand significant total and differential settlement and still perform in a satisfactory manner (Bell *et al.* 1983; Bergado *et al.* 1991, 1994; Bloomfield *et al.* 2001; Curtis *et al.* 1988; Kirschner and Hermansen 1994; Kumada *et al.* 1992; Schlosser and Guilloux 1992). Although a soil wall may perform well on a non-rigid foundation, the general effect of yielding on the behaviour of the wall is not well understood. Previous studies have shown that construction of walls on non-rigid foundations can result in significant base and face deformation of a wall and increased strain in the lower reinforcement layers of a wall (Chou and Wu 1993; Palmeira and Monte 1997; Rowe and Skinner 2001; Schmertmann *et al.* 1989; Yoo and Kim 2001). However, these studies have been limited to the short-term behaviour of the wall, and have been restricted to shallow foundation depths in all but two cases (Rowe and Skinner 2001; Schmertmann *et al.* 1989).

Further, it has been shown that the vertical stress below geosynthetic-reinforced soil walls, irrespective of foundation stiffness, is lower than the estimated design values, except at the toe, where it increases and can be significantly greater than the design value (Allen *et al.* 1992; Bathurst and Benjamin 1990; Bathurst and Simac 1994; Bathurst *et al.* 1989; Berg *et al.* 1986; Bergado *et al.* 1991, 1994; Nakajima *et al.* 1996; Ochiai and Fukuda

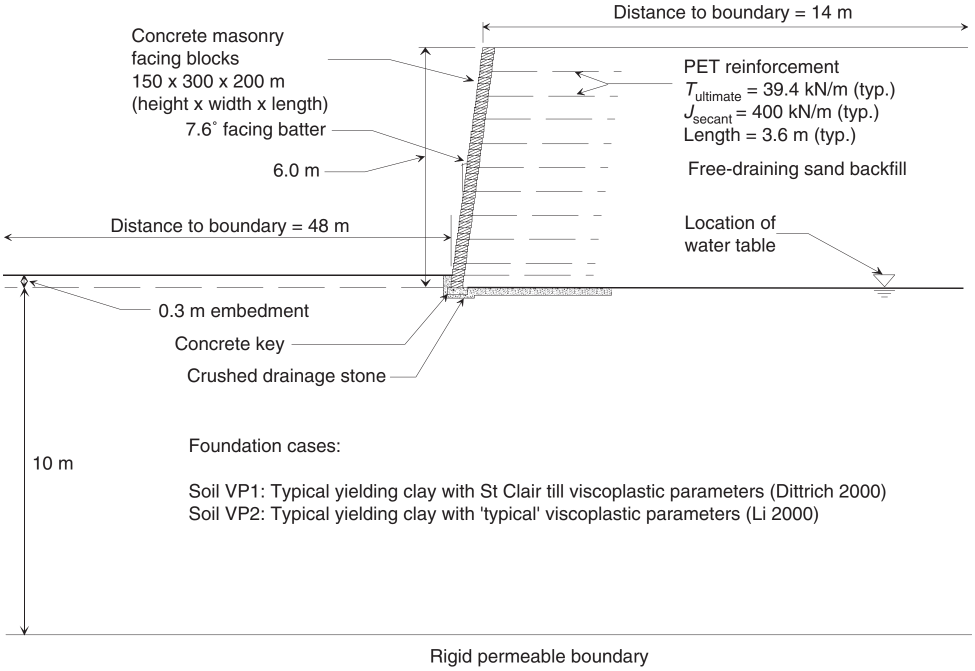

Figure 1. Cross-section of 'typical' wall

1996; Otani *et al.* 1998; Rowe and Ho 1996; Rowe and Skinner 2001; Tsukada *et al.* 1998; Yoo and Kim 2001). However, these previous studies have not considered the effect of the long-term behaviour of the foundation soil and potential redistribution of stresses within the foundation.

A limited number of full-scale test walls have been constructed on various soft to stiff foundations, and in each case the wall was built at, or close to, the expected failure height (based on current design methodologies) (Bell *et al.* 1983; Bergado *et al.* 1991, 1994; Nakajima *et al.* 1996). Although a number of the walls experienced considerable deformations, they all remained stable and no significant signs of distress were detected. Thus, there seems to be a moderate level of conservatism in design methodology that is not fully understood in the case of a geosynthetic-reinforced soil wall constructed on a yielding foundation. Additionally, a number of authors (Bloomfield *et al.* 2001; Kojima *et al.* 1996; Kumada *et al.* 1992) have noted that it is difficult to predict the foundation settlement, and that predicted settlements are often greater than observed deformations. Thus, typical design settlement calculations tend to be overconservative.

A parametric study of a typical 6 m high segmental block-faced geosynthetic-reinforced retaining wall with a sand backfill constructed on a 10 m thick viscoplastic clay foundation was undertaken in order to better understand the effects of a yielding foundation on the behaviour of the reinforced soil wall (Figure 1). The primary objective of the study was to examine the effect of the yielding foundation on the deformations at the top, face and base of the wall, the vertical stress at the base and the horizontal stress behind the face of the wall, and the strain in the reinforcement layers. A secondary objective was to examine the implications of this behaviour with respect to current design methodology (NCMA 1996) in terms of both stability and deformations. The study focuses on the short- and long-term effects for two different foundation cases, the first representing a soil with low viscoplasticity and the second representing a typical viscoplastic material. The reinforced wall examined was designed to meet the required minimum factors of safety (NCMA 1996) for internal and external stability for each foundation case.

2. NUMERICAL MODEL

A version of the finite element (FE) program AFENA originally developed by Carter and Balaam (1990) and modified as noted below to account for both the modelling of geosynthetic-reinforced soil walls and viscoplastic clay behaviour was used to conduct the numerical analyses reported herein. The soil retaining wall was examined under two-dimensional (plane strain) conditions consistent with normal design assumptions (CGS 1992; FHWA 1996; NCMA 1996). The finite element mesh used 3420 eight-noded isoparametric elements to model the soil, masonry and concrete, 200 linear elastic bar elements (with no significant compressive or bending strength) to model the reinforcement, and 1078 interface elements (Figure 2). The interface elements modelled the interaction between the facing blocks and: the reinforcement, the backfill soil, the foundation soil, and each other. Interface elements were also located between the backfill soil and: the reinforcement, and the foundation soil. Finally, interface elements were used between the gravel and concrete key. Details are given in Section 3.1. The initial geostatic stress condition in the foundation was based on the unit weight and effective coefficient of lateral earth pressure at rest (K_0) of the soil.

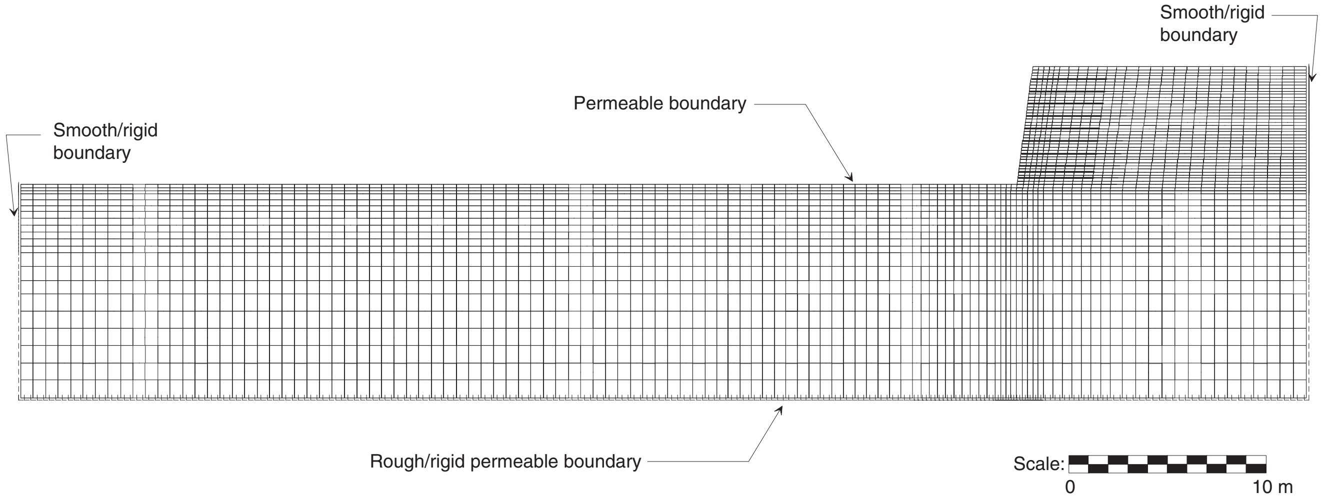

Figure 2. Finite element mesh

The viscoplastic model adopted for the clay foundation continuum elements combined an elliptical yield surface (Chen and Mizuno 1990) and a Drucker–Prager failure criterion with Perzyna's (1963) over-stress model and fully coupled Biot (1941) type consolidation (Rowe and Hinchberger 1998).

An elasto-plastic stress–strain model with a Mohr–Coulomb failure criterion was adopted for the continuum elements used for the coarse-grained soils, masonry facing and concrete key. The Young's modulus, E, of the granular soils was assumed to be non-linear and given by Janbu's (1963) equation expressed in the form

$$\frac{E}{P_a} = K\left(\frac{\sigma_3}{P_a}\right)^n \quad (1)$$

where σ_3 is the minor principal stress, P_a is the atmospheric pressure (e.g. 101.3 kPa), and the values of K and n were selected based on correlations (Duncan *et al.* 1980) with the assumed soil properties. To deal with the case of low σ_3, a minimum stiffness was assumed equal to $K(P_a)^n$. The masonry and concrete materials were assumed to be purely elastic materials.

Rigid-plastic interface elements, as described by Rowe and Soderman (1987), were used to model the behaviour between the various materials. The interface elements were modelled with a stiff spring in each of the shear and normal directions until slip occurred, at which point deformation could occur along the interface and the normal and shear stresses satisfied a Mohr–Coulomb failure criterion based on parameters given in Section 3.1.

The model adopted has previously been used successfully to describe the behaviour of a full-scale reinforced soil wall (Rowe and Skinner 2001), the geosynthetic-reinforced Sackville test embankment (Rowe and Hinchberger 1998), and in the numerical analysis of reinforced embankments constructed on viscoplastic foundation soils (Li 2000; Li and Rowe 1999).

The wall construction was simulated layer by layer following the typical sequence used to build reinforced retaining walls (FHWA 1996). The assumed 24-day construction period and subsequent consolidation analyses were performed in sufficiently small time increments to ensure numerical stability of the solution and to minimise numerical errors.

A limit-equilibrium analysis using Spencer's method (as programmed into Slope/W 2001) was used to examine the global stability of both the wall and the foundation, and it was found that the critical potential slip surface extended around the reinforced soil block and to a depth of approximately 5 m below the base of the wall based on the long-term soil conditions. Thus the foundation was modelled to a total depth of 10 m to ensure an adequate distance between the assumed rough/rigid bottom boundary and the main zone of influence of the construction.

The right and left lateral boundaries were modelled as smooth/rigid. The distance from the front of the wall face to the far boundary was assumed to be greater than 10 times the length of the reinforcement to ensure accuracy in the numerical results (Rowe and Skinner 2001). The distance from the front of the wall face to the slip surface behind the facing was approximated from the limit-equilibrium analysis to be 6 m at the top of the wall. The distance from the wall face to the right smooth/rigid boundary was taken to be more than twice the distance from the front of the wall face to the slip surface behind the facing, to ensure adequate distance between the boundary and the primary zone of influence of the wall. Finally, the top and bottom of the clay layer were assumed to be seepage boundaries allowing two-way drainage of the foundation.

3. DESIGN CONSIDERATIONS AND MODEL PARAMETERS

3.1. Description and design of 'typical' wall

The wall was designed based on the current National Concrete Masonry Association (NCMA) working stress design code (NCMA 1996) for segmental walls. This approach specifically considers a segmental wall facing

Table 1. Geosynthetic material properties

Material property	Test methodology	Value
Ultimate tensile strength (kN/m)	ASTM Standard D 4595	39.7
Creep tensile strength (kN/m)	ASTM Standard D 5262	24.6
Allowable tensile strength (kN/m)	GRI GG4	20.4
Tensile stiffness, J (kN/m)	ASTM Standard D 4595	400

Table 2. Sand and drainage gravel material parameters

Characteristic	Sand backfill	Drainage gravel
Unit weight (kN/m^3)	20	20
Friction angle (degrees)	35	45
Dilation angle (degrees)	6	12.5
Poisson's ratio, μ	0.3	0.35
Coefficient of earth pressure at rest, K_0	0.4	0.3
Janbu K and n	460 and 0.5	900 and 0.7

Table 3. Material interface parameters

Interface	Criterion	Minimum shear force[(a)] (kN/m)	Friction angle (degrees)
Block/block	Ultimate strength	11.5	59
	Serviceability state	9.4	51
Block/reinforcement	Ultimate strength	11.3	20
(pullout strength)	Serviceability state	9.2	22
Backfill/facing block	Ultimate strength	0.0	23.3
Backfill/reinforcement	Ultimate strength	0.0	31.5
Backfill/foundation	Ultimate strength	0.0	27
Gravel/concrete key	Ultimate strength	0.0	30
Embedment/facing block	Ultimate strength	0.0	30

[(a)]Due to block shear key (Bathurst *et al.* 1996a, b); can be reduced to a cohesion by dividing by block width.

and is based on Coulomb's active earth pressure theory. The wall was designed to a height of 6 m with 10 layers of 3.6 m long knitted polyester (PET) geogrid (e.g. Stratagrid 200 from Strata Systems Inc., Cumming, GA, USA). The facing was assumed to be constructed from 40 masonry-facing blocks (e.g. Pisa II blocks from Unilock®, Georgetown, Ontario), each having an infilled unit weight of 21.8 kN/m^3 and a natural setback of 20 mm due to interlocking shear keys. The wall was embedded 0.3 m (Figure 1). A prefabricated concrete key and gravel layer were used at the toe and base of the wall respectively. The concrete key acted as a levelling surface for face alignment only and served no structural purpose. The thin (0.15 m) layer of gravel at the base of the reinforced wall and around the key acted as a level surface for construction of the wall and the top drainage boundary for the clay foundation below the wall. The watertable was assumed to be located at the top of the clay foundation.

The allowable reinforcement tensile strength was assumed to be 20.4 kN/m (as reported by the International Fabrics Association International (IFAI 1999) for Stratagrid 200). This allowable design strength was estimated from the Geosynthetic Research Institute Standards (GRI 1991) based on the ultimate and creep limited tensile strength of the geogrid and accounting for additional reductions in the strength due to installation damage and durability, as indicated in Table 1. The geogrid secant tensile stiffness, J, was taken to be 400 kN/m based on ASTM Standard D 4595 and Bathurst (2000). The polyester geogrid was assumed to have limited susceptibility to creep deformation (Koerner 1990; Rowe 2000).

The reinforced and retained backfill were assumed to be the same cohesionless sand, and the drainage layer at the base of the wall was assumed to be cohesionless gravel. The unit weight, friction and dilation angles, and other assumed parameters for the sand and gravel are given in Table 2. All parameters were taken from the range of typical values for these materials (Craig 1992; Holtz and Kovacs 1981), with the following exceptions. The dilation angle of each material was assumed to be given by Bolton's equation $\psi' = (\phi' - \phi'_{cv})/0.8$ (Bolton 1986), where the value of the constant-volume friction angle (ϕ'_{cv}) was assumed to be 30° and 35° for the sand and gravel respectively (Craig 1992). The non-linear Janbu (1963) stiffness parameters K and n were selected for the assumed soil properties based on Duncan *et al.* (1980).

The block/block and block/reinforcement interface parameters were estimated from test protocol SRWU-1 (NCMA 1996) for both the ultimate and serviceability criteria, as reported by Bathurst *et al.* (1996a, b), and are given in Table 3. The interface friction angle between the facing blocks and the backfill soil was taken as two-thirds the sand friction angle. The same assumption was made for the interface between the gravel soil and both the facing blocks and concrete key based on the gravel material. The interface between the backfill and the foundation was assumed to be equal to the normally consolidated friction angle of the foundation soil, as it was the lesser value for the two soils. The interface friction between the backfill soil and reinforcement was taken as 90% of the backfill friction based on similar material parameters (Krieger *et al.* 1991), rather than the conservative assumption of 70% indicated by NCMA (1996) for the case where no other data are available. The interface friction angles and minimum shear forces between the various materials are summarised in Table 3.

The minimum reinforcement length and wall embedment depth were taken as 0.6 times the height of the wall and the exposed height of the wall divided by 20 respectively, as specified by the NCMA (1996) manual. Further, the maximum reinforcement spacing was limited to twice the facing block width, as recommended by the American Association of State Highways and Transportation Officials (AASHTO 1996). The design coefficient for sliding for the geogrid reinforcement was taken as 0.95 (NCMA 1996).

The NCMA (1996) manual covers a wide range of potential external, internal and facing failure modes, and considers the interface characteristics between the various materials. The internal and facing stability of the wall were governed by the required minimum reinforcement length (3.6 m), the connection strength between the reinforcement and facing blocks for the reinforcement layer second from the base of the wall, and the maximum reinforcement spacing (0.6 m) for the remaining layers. An extra (tenth) layer of reinforcement was added between the original bottom reinforcement layer and base of the wall at a height of 0.3 m to prevent reinforcement/facing connection rupture from occurring in the layer above it. The external stability was based on the assumed foundation conditions discussed below.

3.2. FOUNDATION DESCRIPTION AND DESIGN STABILITY

Three general foundation conditions were considered in this study. The first was a rigid foundation soil considered to represent the standard design and construction conditions, and this served as a baseline for comparison with the other foundation cases. The second and third foundation cases examined were for two stiff clay soils, one with low and the other with typical viscoplastic behaviour, denoted Soil VP1 and Soil VP2 respectively.

The two clay foundation deposits, Soils VP1 and VP2, were assumed to have a liquid limit of 76% and plasticity index of 40%. The initial void ratios and unit weights were taken to be 1.75–1.63 and 15.9–16.3 kN/m^3 for Soil VP1, and 2.0–1.75 and 15.6–16.0 kN/m^3 for Soil VP2 (from top to bottom of the deposit). The vertical hydraulic conductivity of the clay foundations was assumed to be a function of the void ratio given by the equation

$$k_v = k_{v0} \times \exp\left(\frac{e - e_0}{C_k}\right) \tag{2}$$

where the initial hydraulic conductivity (k_{v0}) and initial void ratio (e_0) are given in Table 4 and the hydraulic

Table 4. Foundation material properties

Property	Soil VP1	Soil VP2
General soil properties:		
Specific gravity	2.74	2.74
Liquid limit (%)	76	76
Plasticity index	40	40
Compression index, C_c	0.69	0.69
Recompression index, C_r	0.069	0.069
N/C friction angle (degrees)	27	27
N/C cohesion (kPa)	0	0
O/C friction angle (degrees)	20	20
Coefficient of earth pressure at rest, K_0	0.6	0.6
Poisson's ratio, μ	0.35	0.35
Elliptical cap aspect ratio, R_c	1.2	1.2
Initial hydraulic conductivity, k_{v0} (m/s)	1×10^{-9}	1×10^{-9}
Ratio of horizontal to vertical hydraulic conductivity, k_h/k_v	3	3
Case-specific soil properties:		
Fluidity constant (h^{-1})	3.6×10^{-3}[(a)]	1.0×10^{-7}[(b)]
Strain rate exponent	70[(a)]	30[(b)]
Initial void ratio (top to bottom of deposit)	1.75–1.63	2.0–1.75
Average unit weight (kN/m^3)	16.1	15.8
Preconsolidation pressure at top of layer (kPa)	171	93
Change in preconsolidation pressure with depth (kPa/m)	4.5	4.5
Undrained shear strength at top of layer[(c)] (kPa)	51.6	50.3
Change in undrained shear strength with depth[(c)] (kPa/m)	0.3	0.9

[(a)]Dittrich (2000).
[(b)]Li (2000), estimated from Kulhawy and Mayne (1990).
[(c)]Based on the estimated corrected (Bjerrum 1973) shear vane results.

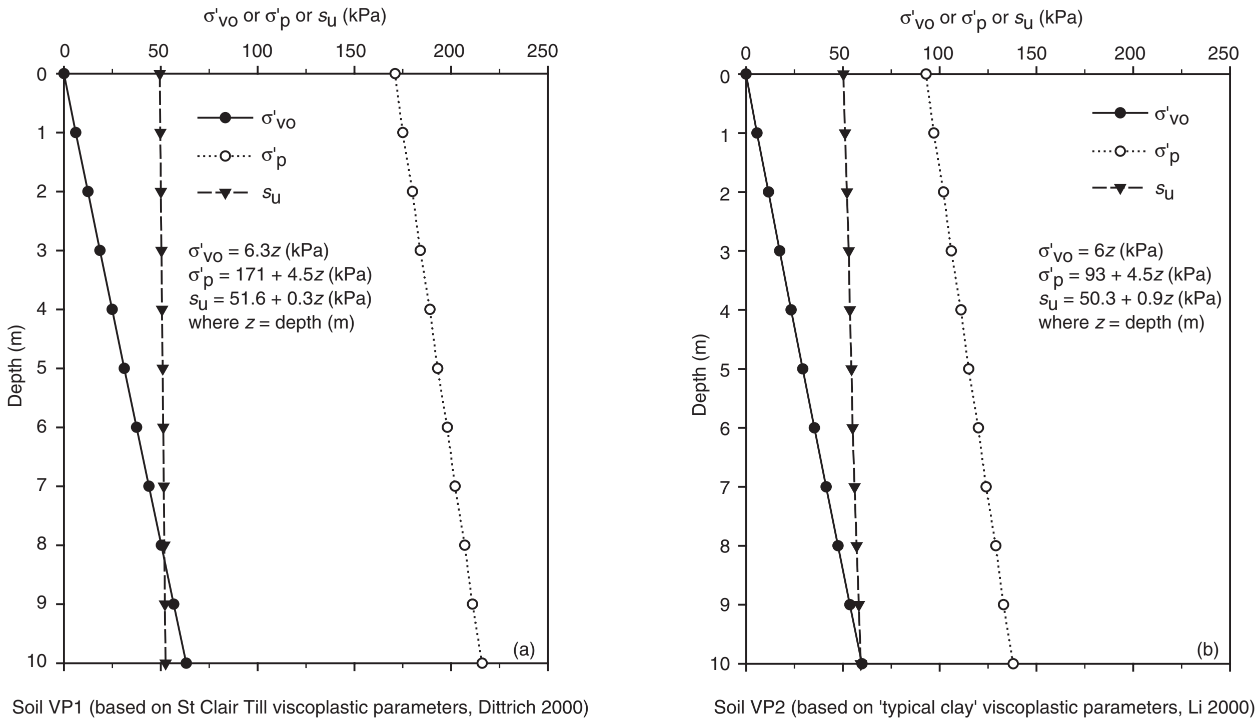

Figure 3. Initial effective stress, preconsolidation pressure and undrained shear strength of foundation cases (s_u = Bjerrum (1973) corrected shear vane strength)

conductivity change index (C_k) was taken to be 0.5 for both cases (based on Mesri *et al.* 1994). Recognising that typically the hydraulic conductivity of clay is anisotropic (Tavenas *et al.* 1983; Terzaghi *et al.* 1996), the ratio of horizontal to vertical hydraulic conductivity was assumed to be $k_h/k_v = 3$. The viscoplastic characteristics of Soil VP1 were based on the slightly rate-sensitive behaviour of the St Clair till examined by Dittrich (2000), whereas the more viscous behaviour of Soil VP2 was based on the rate-dependent relationship between undrained shear strength and strain rate presented by Kulhawy and Mayne (1990) using viscoplastic parameters established for this case by Li (2000). All other relevant soil properties used in this study for Soils VP1 and VP2 are summarised in Table 4. The initial vertical effective stress and preconsolidation pressure profiles for Soils VP1 and VP2 are shown in Figure 3, and it can be seen that Soil VP1, with the low viscoplastic behaviour, had a higher preconsolidation pressure profile. Based on these parameters (including the viscoplastic nature of the soils), and accounting for the relationship between plane strain and corrected (Bjerrum 1973) field vane strengths (Skinner 2002), the corrected undrained shear vane strength at the top of the foundation stratum, s_{u0}, was calculated for Soil VP1 to be 51.6 kPa, increasing with depth at a rate of 0.3 kPa/m, and for Soil VP2 to be 50.3 kPa, increased with depth at a rate of 0.9 kPa/m. The undrained shear vane strength profiles for Soils VP1 and VP2 are shown in Figure 3.

For this study, it was found that the external stability was governed by the short-term bearing capacity analysis. The method of bearing capacity analysis specified by the NCMA (1996) considers the reinforced soil wall to act as a rigid block, with a reduced bearing area due to eccentricity. The short-term ultimate bearing capacity of the foundation was estimated from the corrected (Bjerrum 1973) field vane shear strength profile and the bearing capacity solutions published by Davis and Booker (1973), and a factor of safety for bearing capacity of 2.0 was achieved for both foundations.

Thus Soils VP1 and VP2 had slightly different corrected undrained field vane shear strength profiles due to their different viscoplastic natures, but did have the same short-term bearing capacity for this case. The soils also had the same long-term cohesion and friction angle strength characteristics. However, owing to the more viscous nature of Soil VP2 compared with Soil VP1, its undrained shear strength was more sensitive to changes in strain rate. Thus Soil VP2 had a higher potential for generation of additional excess porewater pressure after the end of construction, viscoplastic yielding, and secondary consolidation (creep) than Soil VP1.

4. RESULTS OF ANALYSIS

4.1. General

When comparing the three foundation cases, recall that the first was assumed to be rigid such that there were no significant long-term deformations, and that the second and third cases (Soils VP1 and VP2) were both assumed to be stiff clays with different viscoplastic behaviour. In general, Soil VP1 had relatively low viscoplastic behaviour and a higher preconsolidation (σ'_p) profile than Soil VP2. Soil VP1's higher σ'_p profile meant that the foundation was more overconsolidated, stiffer and therefore less compressible than Soil VP2 under the same loading conditions.

It should be noted that the degrees of consolidation (i.e. 95% consolidation) discussed in this study are for a point along the right lateral boundary in the middle of the foundation deposits (i.e. halfway between the top and bottom drainage boundaries). The associated average degree of consolidation along the right lateral boundary was slightly greater than the given magnitude in each case (for example, 95% degree of consolidation at the reference point corresponded to an average degree of consolidation of 97%). The magnitude of consolidation at this point has been used in this study to represent the lowest magnitude at any given time within the clay foundation deposit.

In addition, Soils VP1 and VP2 were compared at the end of construction (EOC), one year after the EOC when case VP1 had reached 95% (average degree of) consolidation (case VP2 was at 20% consolidation), and seven years when case VP2 had reached 95% consolidation (case VP1 had reached 99% consolidation). Although it was possible for the viscoplastic clay deposits to generate additional excess porewater pressure within the clay foundation after the end of construction, this did not significantly affect the magnitude of the average degree of consolidation in this study.

4.2. Comparison of rigid and compressible foundation conditions

A comparison of the vertical and horizontal displacements calculated for the rigid foundation and the significantly more compressible (but stiff) foundation Soils VP1 and VP2 shows that the deformation at the face and base of the wall were considerably higher for Soils VP1 and VP2 (Figures 4 and 5) than for the rigid foundation. (In the following discussion all increases mentioned are relative to those calculated for a rigid foundation.) Increased deformation at the base was expected for Soils VP1 and VP2; however, the maximum settlement was over 35 mm and 200 mm across the base of the wall at the EOC and approximately 95% consolidation respectively for Soil VP2. The increased foundation deformation contributed significantly to the

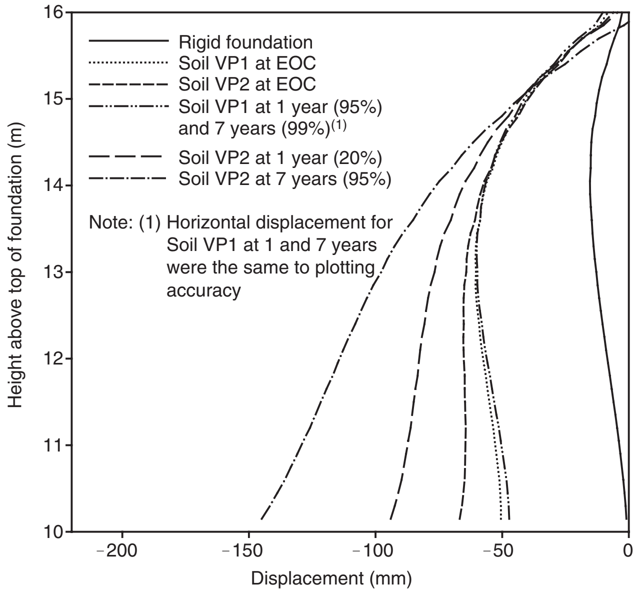

Figure 4. Horizontal displacements at wall face (EOC = end of construction; 20%, 95% and 99% = percentage degree of consolidation at a point along right lateral boundary at centre of foundation deposit)

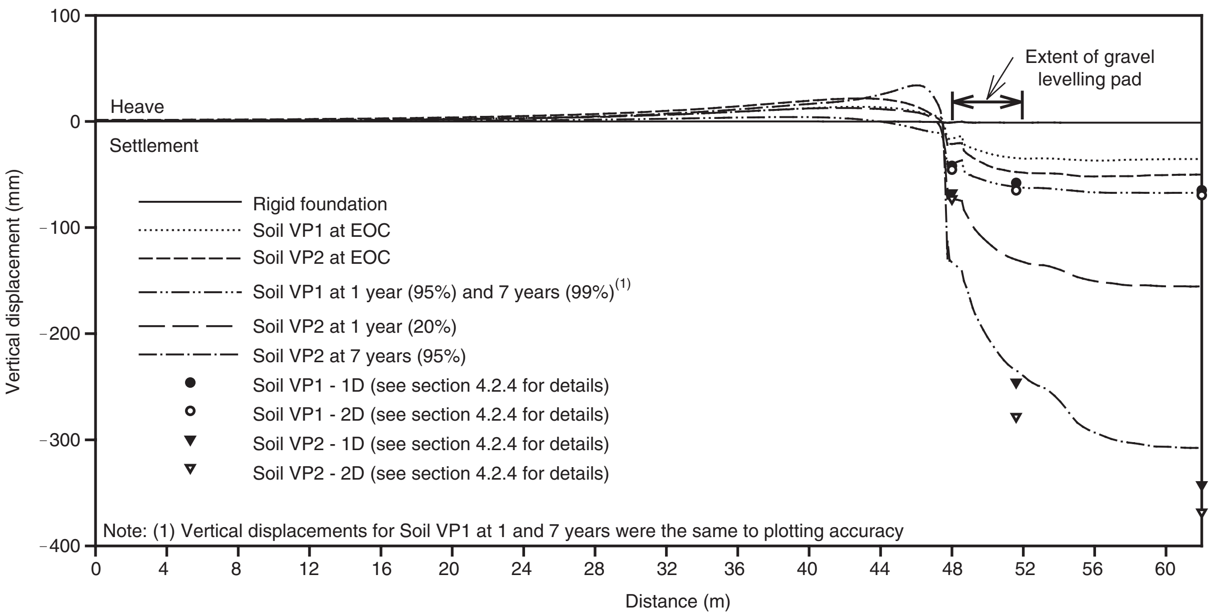

Figure 5. Vertical displacement along top of foundation (EOC = end of construction; 20%, 95% and 99% = percentage degree of consolidation at a point along right lateral boundary at centre of foundation deposit; 1D and 2D = one- and two-dimensional hand-calculated settlement)

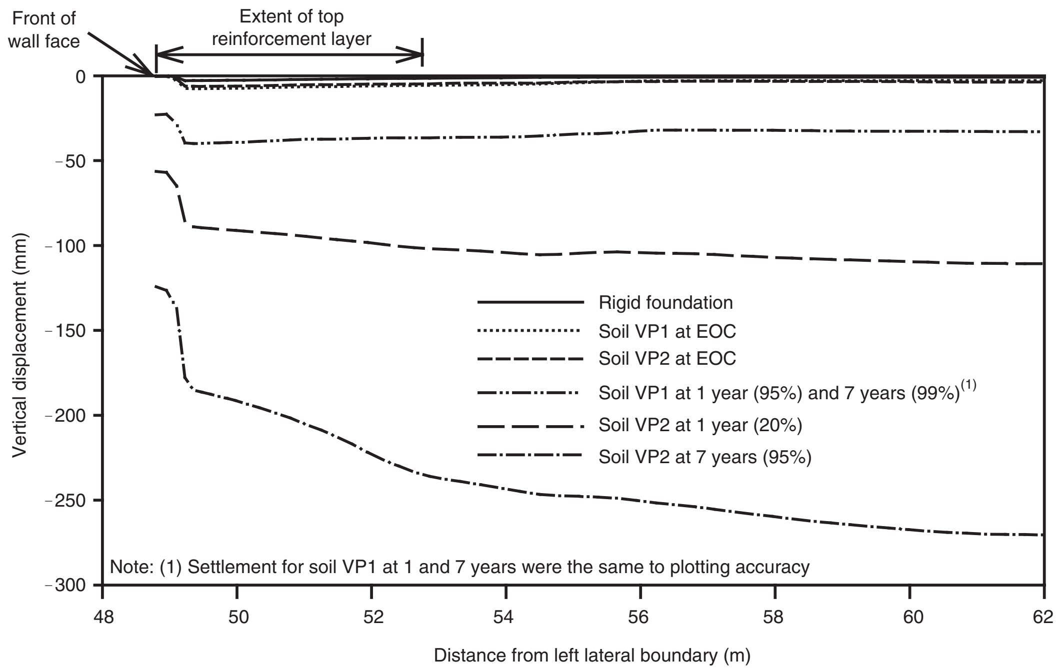

Figure 6. Vertical displacement at top of wall (EOC = end of construction; 20%, 95% and 99% = percentage degree of consolidation at a point along right lateral boundary at centre of foundation deposit)

facing displacement, and caused more rotational movement about the top of the wall face, with the maximum displacement increasing by 40 mm and 130 mm at the EOC and approximately 95% consolidation respectively for Soil VP2. It should be noted that these deformations might exceed case-specific serviceability limits that were not considered in this study. The very slight backward rotation of the wall face from the EOC to 95% consolidation for case VP1 was caused by local displacements at the face and especially at the toe of the wall. The significant deformations at the face and base resulted in increased vertical displacements at the top and higher strains in the reinforcement layers throughout the height of the wall for Soils VP1 and VP2 (Figures 6 and 7). The deformations along the top of the wall increased by more than 200 mm, and the maximum strain in the reinforcement layers increased between 90% and 230% at approximately 95% consolidation for Soil VP2 relative to the rigid foundation case. The slightly higher reinforcement strain in the lowest layer (height = 0.3 m) at the EOC for case VP1 compared with VP2 was due to the slightly larger deformation for the reinforced soil block itself for case VP1; even though the displacements at the base and face of the wall were greater for case VP2 the reinforced soil block tended to move with the foundation. Owing to stress redistribution within the foundation, the calculated vertical stresses at the toe of the wall for the compressible foundation cases were less than half that for the rigid case (Figure 8).

Although significant deformations were calculated from the FE analysis reported herein, it has been shown by Gnanendran (1993) that accounting for geometric non-linearity in the FE analysis (via large-

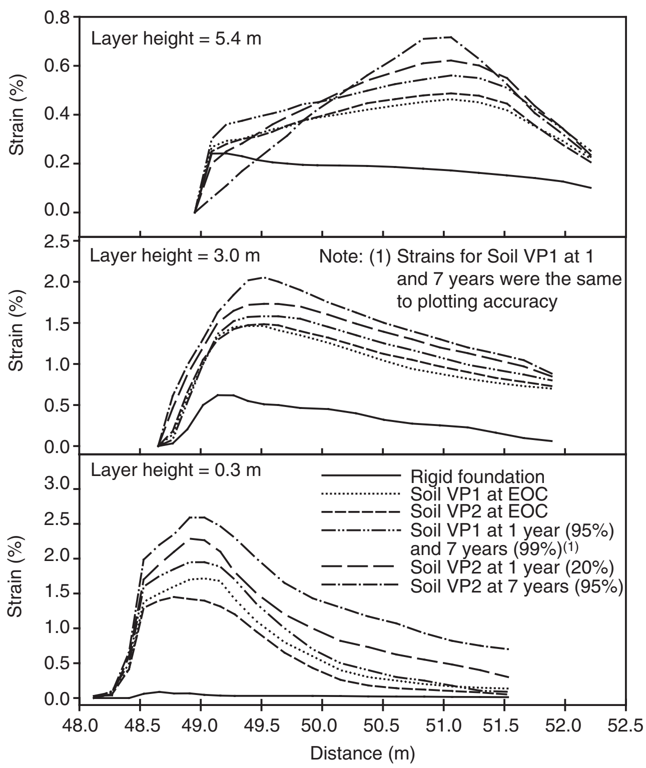

Figure 7. Strains at various layers of reinforcement (EOC = end of construction; 20%, 95% and 99% = percentage degree of consolidation at a point along right lateral boundary at centre of foundation deposit)

strain analysis) of the construction of embankments on similar yielding foundation conditions does not significantly affect the results of the analysis until the collapse load of the foundation is approached.

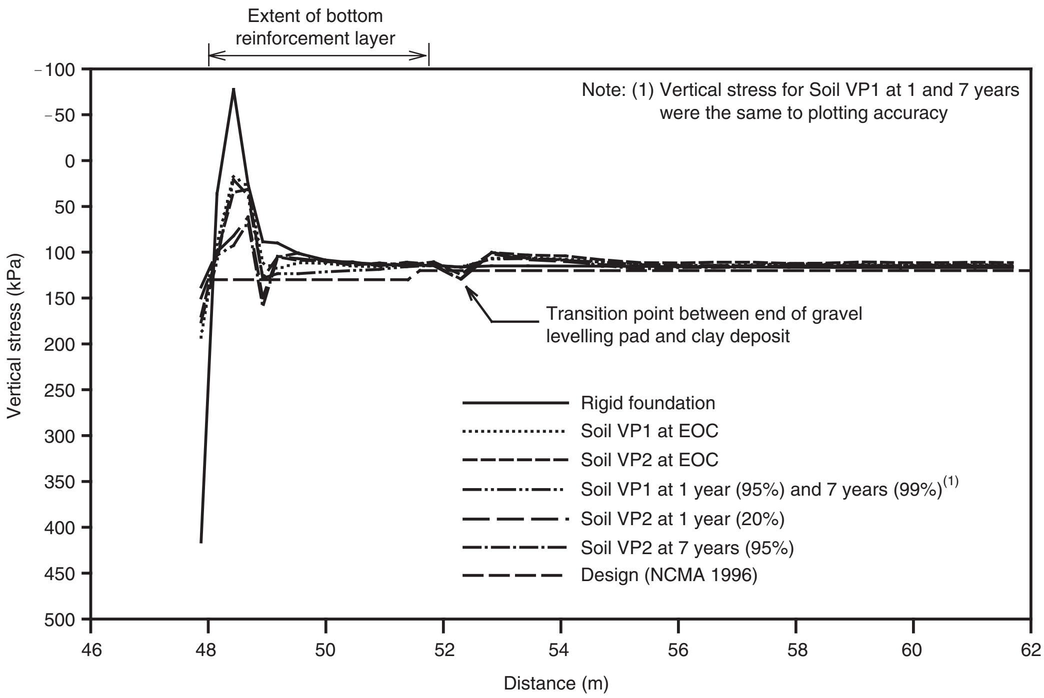

Figure 8. Vertical stress at base of wall (EOC = end of construction; 20%, 95% and 99% = percentage degree of consolidation at a point along right lateral boundary at centre of foundation deposit)

The general trends noted above are consistent with previous studies comparing rigid and compressible foundations (Chou and Wu 1993; Palmeira and Monte 1997; Rowe and Skinner 2001; Schmertmann *et al*. 1989; Yoo and Kim 2001). However, this previous body of research was limited to the short-term behaviour of the wall and foundation. Accounting for the long-term behaviour of cases Soils VP1 and VP2 showed that, along with increased deformations at the base, the displacements at the face and top of the wall and the reinforcement strains continued to increase with time owing to continued primary and secondary settlement. As these increases are not currently considered in design, the long-term behaviour of each case was compared and is discussed below.

4.3. Comparison of various viscous foundation conditions

The results of the analyses with Soil VP1 were compared with those of the significantly more viscous Soil VP2, at the EOC and at the time of approximately 95% consolidation. For the lower viscosity Soil VP1 there was no significant change in behaviour between the time of 95% consolidation (reached one year after the EOC) and subsequent times (e.g. seven years). The more viscous Soil VP2 reached approximately 20% consolidation one year after the EOC, and approximately 95% consolidation seven years after the EOC.

4.3.1. *General wall and foundation behaviour*

At the end of construction, the distributions of soil movement within the backfill and clay foundation were approximately the same for Soils VP1 and VP2. The majority of the soil directly below the wall was in an overconsolidated (O/C) state of yield at the end of construction for both cases. With subsequent time and consolidation, the soil moved below the yield surface to an elastic state in the case of Soil VP1, and into a normally consolidated (N/C) yield state in the case of Soil VP2. These changes can be illustrated by examining the stress paths at a point 3 m below the toe of the wall (Figure 9). For Soil VP1, the stress path reaches the O/C yield surface by the EOC and as time and consolidation progress, the stress path moves towards the N/C yield surface but remains within the elastic range. For Soil VP2, the stress path goes outside the long-term O/C yield surface due to the soils more viscous nature and with subsequent time the stress path moves into the N/C range above the initial static yield surface.

The more viscous nature of Soil VP2 compared with Soil VP1 contributes to greater time-dependent behaviour of the soil. The lower viscosity Soil VP1 had a higher preconsolidation pressure profile than Soil VP2 for a soil profile corresponding to the same minimum bearing capacity factor of safety of 2.0. The lower preconsolidation pressure profile of Soil VP2 resulted in a lower overall stiffness than for Soil VP1, which greatly influenced the behaviour of the foundation and specifically the displacements of the wall.

4.3.2. *Reinforcement strains and vertical stress at base of wall*

Soil VP2 produced higher overall strains in the reinforcement layers at the EOC, and one year and seven years after the EOC (Figure 7), and showed a greater increase in the maximum strain over time than Soil VP1. The maximum reinforcement strain increased by 10%, 7% and 22% at the heights of 0.3, 3.0 and 5.4 m respectively between the EOC and one year (95%

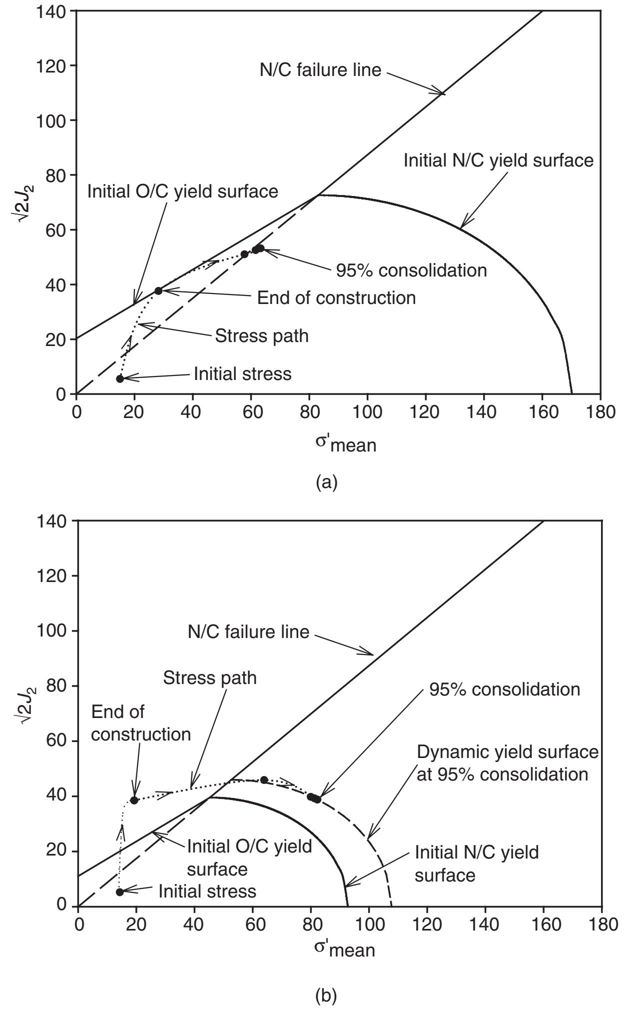

Figure 9. Stress paths at point 3.0 m below toe of wall for: (a) Soils VP1; (b) Soil VP2

consolidation) for Soil VP1. For the same heights, the maximum strains increased by 64%, 13% and 29% respectively between the EOC and one year for Soil VP2, and continued to increase by 13%, 18% and 13% respectively between one year and seven years (95% consolidation). These increases in strain can be attributed to the consolidation settlement and yielding of the foundation for both cases.

The model considered time-dependent deformation both during primary consolidation and subsequently. However, it was found that for Soil VP1, the time-dependent deformations were predominantly due to primary consolidation with little or no secondary consolidation or yielding after the EOC. In contrast, the base displacements (discussed below) and increases in reinforcement strain for Soil VP2 were due to a combination of primary and secondary consolidation and yielding of the foundation soil. Although the significant increases in reinforcement strain for both cases would not be accounted for in current design, at no time was the strain greater than the maximum allowable reinforcement strain (5% in this case), and thus the time-dependent increase in strain could be accommodated by the conservative nature of the design in this case. However, it was found that the forces (and associated strains) in the reinforcement layers were between 13% and 45% higher (from the bottom to the top reinforcement layer respectively) than the design (NCMA 1996) value at 95% consolidation for Soil VP2 (where both the FE and design strain values were based on the assumed reinforcement secant stiffness modulus of 400 kN/m). Had the internal stability been governed by the reinforcement strength, and had the resulting magnitude of the reinforcement layer forces been close to the allowable design limit, then the time-dependent increase in strain (and force) due to the viscoplastic foundation behaviour could have led to an inadequate design, not accounting for the intrinsic conservatism of current design methods (Allen and Bathurst 2002).

Due to its lower stiffness, Soil VP2 gave rise to lower values of the maximum vertical stress at the toe of the wall (Figure 8) than Soil VP1. For both cases the predicted maximum vertical stress at the toe was greater (approximately 30%) than the assumed design (NCMA 1996) value at all times, but did decrease slightly (approximately 10%) with time, probably as a result of stress redistribution in the foundation. It should be noted that the slightly jagged shape of the vertical stress at approximately the 52 m location for all cases was due to the transition in soil materials below the wall backfill from the end of the gravel levelling pad to the clay foundation deposit. The slight increase in the vertical stress at these locations may be attributed to stresses arching to the stiffer gravel material from the clay.

4.3.3. *Stability*

The wall met the specified minimum factors of safety for internal and external stability for both foundations based on the corrected shear vane strength profile of each case. However, this conventional approach did not provide any consideration of the effect of the viscoplastic nature of the soil during or after construction. The viscoplastic nature of the soil could result in instability of the foundation due to a lower undrained shear strength at the induced strain rates at the end of construction relative to those in the field vane test.

The FE analysis showed that at no time was either foundation soil unstable because of the applied wall load, and there was no significant excess porewater pressure generation after the end of construction. Accounting for the approximate strain rates in the foundation below the wall at the end of construction, the undrained shear strength profiles and associated factors of safety were calculated. The factors of safety for Soils VP1 and VP2 were 1.8 and 1.5 respectively. These were both less than the initial design value of 2.0, but much greater than unity and therefore stable. However, this illustrates the importance of considering the effect of construction strain rate for viscous soils, and shows that the conventional method of estimating the ultimate bearing capacity from the corrected field vane strength profile may not reflect the potential decrease in undrained shear strength that could occur. The maximum shear strains (and associated shear stresses) occurred at the toe of the wall at both the end of construction and at approximately 95% consolidation and highlights the importance of toe stability, which is not normally considered in design. The stability of the toe can be accounted for in design by considering the local bearing capacity of the lowest structural element along the face (either the bottom facing block or the concrete key if one has been used, as in this case). The concrete key can be assumed to act as a shallow strip footing with an applied load equal to the applied vertical stress considered in design (NCMA 1996) for the bearing capacity of the entire reinforced soil block. The applied vertical stress may be increased by 30% for toe stability, as discussed in Section 4.2.2, but it should be noted that the percentage increase was based on this case alone, and further investigation is required for a larger number of cases.

4.3.4. *Settlement*

The settlements of both cases (Soils VP1 and VP2) were approximately the same up to the end of construction, with the exception of slightly higher displacements for Soil VP2 due to its more viscous nature and lower stiffness (Figures 4–6). After the end of construction, Soil VP2 gave higher total displacements and differential settlements compared with Soil VP1 at one and seven years. These differential settlements were of 50 mm and 100 mm at the top and base of the wall respectively. These large foundation settlements resulted from the combined effects of the primary and secondary consolidation and viscoplastic shear deformations of the soil (Figure 9). The total and differential settlements could be in excess of allowable project specifications for Soil VP2. In the less viscous case (Soil VP1), the horizontal displacement of the wall face had a more traditional 'bulge' profile, indicative of a segmental facing wall constructed on a relatively competent foundation (Allen *et al.* 1992; Bathurst and Simac 1994; Nakajima *et al.* 1996; Wu 1992a,b), and did not significantly change between the EOC to seven years (99% consolidation). For the viscous case (Soil VP2), the wall rotated about its top, and the maximum face displacement occurred at the toe. Furthermore, the maximum facing displacement increased by 120% between the EOC and seven years (95% consolidation), primarily due to creep resulting from the viscous nature of foundation Soil VP2.

A number of authors (Bloomfield *et al.* 2001; Kojima *et al.* 1996; Kumada *et al.* 1992) have noted that it is difficult to predict the settlement of a reinforced soil wall constructed on a yielding foundation, and in a number of cases the predicted settlements were significantly greater than the observed deformation. Therefore a comparison of the typical one- and two-dimensional (denoted in the following as 1D and 2D respectively) settlement calculations with those from the FE analysis is presented (Figure 5). The 1D and 2D consolidation settlements were estimated from the traditional hand-calculated strain integration method and based on the assumed soil parameters. The 1D and 2D vertical strains were estimated from Davis and Poulos (1968), accounting for the initial stress-dependent elastic stiffness of the soils and the change in stress from the O/C to the N/C range due to loading beyond the preconsolidation pressure (Skinner 2002). The settlement was estimated at three points along the base of the wall: the toe, the end of the reinforced soil zone, and the right boundary. For the purposes of hand calculation the wall was assumed to behave as an infinite strip footing on a foundation of finite depth, and the associated increases in stress were estimated from Poulos and Davis (1974), accounting for the right boundary as a line of symmetry. The vertical load at the toe of the wall was increased by 30% to account for the transfer of forces from the reinforcement to the wall face, as discussed earlier, and the associated horizontal loads, as estimated from Poulos and Davis (1974), were increased in proportion.

The hand-calculated 1D and 2D settlements for Soil VP1 both compared reasonably well with the FE deformations at approximately 95% consolidation (one year). The 1D estimates tended to underestimate and the 2D estimates to overestimate the FE deformation, but the difference between the hand-calculated and FE predictions was less then 5%, except at the end of the reinforcement for the 1D case (7% difference) and at the toe of the wall for the 2D calculation (14% difference). These slight variations were attributed to the approximation associated with representing the applied loading conditions and the moduli.

The estimated 1D and 2D settlements for Soil VP2 compared only moderately well with the predicted FE deformations along the base of the wall at approximately 95% consolidation (seven years). The estimated 1D and 2D settlements underpredict the FE deformations at the toe of the wall, by 50% and 46% respectively, and overpredict the FE deformations by between 5% and 20% at the end of the reinforcement and the right boundary, with the 2D method yielding the larger differences. The differences between the hand-calculated and FE results at all three of the points were again attributed to the approximation associated with representing the applied loading and the moduli. However, the significantly greater differences between the two methods at the toe of the wall were also due, in part, to the hand-calculation method predicting that only O/C behaviour would occur, whereas more compressible N/C behaviour was predicted in the FE analysis. This is due to the fact that the hand-calculation method bases the change in behaviour from the O/C to the N/C range on the change in vertical stress and initial preconsolidation pressure alone, whereas the FE method accounts for the three-dimensional change in stress, and tracks the stress path of the soil to account for when it passes beyond the initial O/C and N/C yield surfaces. Additionally, and to a lesser degree, the difference between the hand and FE methods may also be due to the viscoplastic shear behaviour predicted at the toe of the wall in the FE analysis, which was not accounted for in the hand-calculations.

Therefore, accounting for the 2D changes in stress due to loading, the increased load at the toe of the wall due to transfer of stresses from the reinforcement and backfill soil and the stress-dependent O/C stiffness yielded good to fair estimates of the predicted deformations for both the 1D and 2D methods for Soils VP1 and VP2. Although neither of the hand-calculated settlement methods could directly take account of the viscoplastic nature of the soil, the estimated moduli seemed to underestimate the overall stiffness of the soil, and thus slightly overestimate the majority of the settlement below the wall in this study. This is with the exception of the point at the toe of the wall for Soil VP2, where the difference between the two methods of estimating the point at which N/C behaviour occurs significantly influenced the results and led to underestimation of the predicted FE deformations.

5. PARAMETRIC STUDY OF VISCOUS FOUNDATION ANALYSIS

5.1. General

A parametric study was conducted to investigate the effects of varying the hydraulic conductivity and construction rate on the stability and behaviour of the wall over Soil VP2.

5.2. Initial vertical hydraulic conductivity

The initial vertical hydraulic conductivity (k_{v0}) of 1×10^{-9} m/s was decreased by a factor of 10 to 1×10^{-10} m/s, and the analysis was re-run to 95% consolidation. This would allow for larger potential increase in the excess porewater pressure after the end of construction to occur and decrease the overall stability of the foundation, as has been observed in the field (Rowe and Hinchberger 1998). The time to 95% consolidation increased from seven years for the original analysis to 55 years for the lower value of k_{v0}. This increase in consolidation time allowed for additional settlement (the combination of primary and secondary consolidation) to occur. However, slower dissipation of the initial and post-construction excess porewater pressures due to the decrease in hydraulic conductivity had no other noticeable effect on the overall stability and behaviour of the wall and foundation.

5.3. Construction rate

The effect of increasing the time of construction from the initial assumed value of 24 days to 120 days was also examined. The corresponding lower strain rate in the foundation decreased the mobilised undrained shear strength (by approximately 13% compared with the shear strength for the base rate of construction), but had no significant effect on the results of the analysis, and the wall and foundation remained stable. Although the decrease in strength did not lead to a significant change in behaviour, the bearing capacity factor of safety was reduced from 1.5 to 1.3, showing that the rate of construction should be considered in any viscoplastic foundation case.

5.4. Initial vertical hydraulic conductivity and construction rate

An analysis combining the decrease in both the hydraulic conductivity and construction rate (by factors of 10 and 5 respectively) was conducted to investigate the stability and behaviour of the wall. It was found that the wall and foundation were stable at all times during the analysis and behaved as expected based on the previous observations for the individual cases. The estimated strain rates in the foundation during construction were found to decrease, thus slightly decreasing the undrained shear strength of the soil. The time to 95% consolidation increased from 7 to 55 years and subsequently increased the overall settlements of the wall at 95% consolidation owing to the greater time for creep deformations to occur. Nevertheless, as the wall was originally designed with adequate external factors of safety, this was sufficient to accommodate the decrease in foundation strength in this case.

6. SUMMARY AND CONCLUSIONS

The behaviour of a reinforced soil wall constructed on a yielding foundation is not well understood or considered in current design methods, and this is the first investigation to examine the long-term effects of a yielding foundation on the behaviour of a soil wall. The results of finite element analyses of a typical reinforced soil wall constructed on rigid, low-viscosity and moderate-viscosity foundation soils have shown that the viscoplastic behaviour of some fine-grained soils can potentially cause lower undrained shear strength and external stability than predicted from conventional design analysis. For the cases examined, it was found that the mobilised undrained shear strength of the foundation decreased (by 20%) due to the strain rate dependent nature of the soil, and lowered the factor of safety for bearing capacity (to 1.5 for Soil VP2). However, the minimum design factor of safety of 2.0, based on the corrected field vane shear strength, was sufficient to accommodate this decrease in strength and ensure the stability of the wall. If a lower minimum required factor of safety is used in design on a viscous foundation, failure could potentially occur and thus the strain rate sensitive undrained shear strength of a yielding foundation should be considered in design.

It was found that the vertical stress along the bottom of the reinforced wall was less than the expected design value except at the toe. Accounting for the observed decrease in vertical stress at the toe with time due to stress redistribution, the maximum stress at the toe was on average 30% greater than the design value in this case. Although this increase may be valid for this case, further investigation is required before this 30% increase is generalised. The stability of the toe should be considered in design by accounting for the local bearing capacity of the lowest structural element along the wall face and the increased applied vertical stress.

It was shown that a viscous foundation soil may lead to significant total and differential settlements of a structure, depending on the preconsolidation pressure profile and applied loading. If the applied loading is sufficient to increase the effective vertical stress beyond the preconsolidation pressure and into a normally consolidated state, then considerable viscoplastic consolidation and yielding settlements could occur. Increased settlement can lead to higher strains and forces in the reinforcement layers, potentially greater than the expected design values, and facing and base deformations that could exceed allowable project design limits at both the end of construction and 95% consolidation. Relative to a wall on a rigid foundation, the maximum reinforcement strain increased by more than 200% and as much as 85% between the EOC to 95% consolidation for a yielding foundation. Although no reinforcement strains reached the maximum allowable design limit in the case examined, it was shown that the strains were 13% (bottom layer) to 45% (top layer) greater than the expected design (NCMA 1996) values. Thus the increase in reinforcement strain due to a yielding foundation condition can lead to underestimating the reinforcement strains, and should be accounted for in design.

It is difficult to estimate the maximum deformation of the wall face as it is dependent on the type of facing system used, and on the stiffness of the reinforcement and backfill materials. For this case, it was found that the maximum horizontal displacement of the face at 95% consolidation was 130 mm more for the viscous foundation than for the rigid foundation.

It has been previously found that traditional 1D settlement calculations may significantly overestimate the settlements at the base of the wall. It was shown that simple 1D and 2D strain integration calculations that consider the stress history of the soil, the applied 2D loading, the increased stress at the toe, and the stress-dependent elastic stiffness gave good to fair predictions of the settlement below the wall in this case. This is with the exception of the toe of the wall, where the difference between the hand-calculated and FE methods of predicting the point at which N/C behaviour begins led to the hand-calculated values significantly underestimating the predicted FE deformations. Although these methods may be valid for this case, further investigation of different loading cases should be conducted for comparison.

Decreases in the hydraulic conductivity and construction rate can potentially cause failure of a viscoplastic foundation by decreasing the dissipation rate for the initial and post-construction excess porewater pressure and decreasing the undrained shear strength during construction. However, for the cases examined, it was shown that a bearing capacity factor of safety of 2.0 based on conventional design was sufficient to account for these additional potential instabilities in the foundation soil, and the wall was stable at all times during the analyses. This does not mean that the viscoplastic affects of a foundation soil should be neglected in design, and careful consideration should be given to the effect of strain rate when assessing the factor of safety for external bearing capacity.

ACKNOWLEDGEMENTS

The research reported herein was funded by the Natural Sciences and Engineering Research Council of Canada (NSERC) and the Ontario Ministry of Training, Colleges and Universities in the form of an Ontario Graduate Scholarship. The constructive comments of the reviewers were much appreciated.

NOTATIONS

Basic SI units are given in parentheses.

C_c	compression index (dimensionless)
C_k	hydraulic conductivity change index (dimensionless)
C_r	recompression index (dimensionless)
E, E'	Young's modulus of elasticity (Pa)
E_c	one-dimensional confined modulus (Pa)
$E_{c\text{-}o/c}$	initial O/C elastic stiffness (Pa)
e	void ratio (dimensionless)
e_0	initial void ratio (dimensionless)
J	geogrid secant tensile stiffness (N/m)
K	material constant of Janbu's model (dimensionless)
K_0	coefficient of earth pressure at rest (dimensionless)
k_h	horizontal hydraulic conductivity (m/s)
k_v	vertical hydraulic conductivity (m/s)
k_{v0}	initial vertical hydraulic conductivity (m/s)
n	material constant of Janbu's model (dimensionless)
P_a	atmospheric pressure (Pa)
R_c	elliptical cap aspect ratio (dimensionless)
s_{u0}	initial corrected undrained shear strength at top of deposit (Pa)
ν	Poisson's ratio (dimensionless)
σ_3	minor principal stress (Pa)
σ'_p	preconsolidation pressure (Pa)
ϕ'	friction angle (°)
ϕ'_{cv}	constant-volume friction angle (°)
ψ'	dilatancy angle (°)

REFERENCES

AASHTO (1996). *Standard Specifications for Highway Bridges, with 1998 Interims*, 16th edn, American Association of State Highway and Transportation Officials, Washington, DC.

Allen, T. M. & Bathurst, R.J. (2002). Observed long-term performance of geosynthetic walls and implications for design. *Geosynthetics International*, **9**, Nos 5–6, 525–566.

Allen, T. M., Christopher, B. R. & Holtz, R. D. (1992). Performance of a 12.6 m high geotextile wall in Seattle, Washington. *Geosynthetic-Reinforced Soil Retaining Walls*, Wu, J. T. H., Editor, Balkema, Rotterdam, pp. 81–100.

ASTM D 4595 (1998). *Standard Test Method for Tensile Properties of Geotextiles by Wide-Width Strip Method*, American Society for Testing and Materials, West Conshohocken, PA, USA.

ASTM D 5262 (1998). *Standard Test Method for Evaluating the Unconfined Tensile Creep Behaviour of Geosynthetics*, American Society for Testing and Materials, West Conshohocken, PA.

Bathurst, R. J. (2000). Unpublished test data for ASTM Standard D 4595 Stress–strain Data for Stratagrid 200. Obtained from

Dr R. Bathurst, Royal Military College, Kingston, Ontario, Canada.

Bathurst, R. J. & Benjamin, D. J. (1990). Failure of a geogrid-reinforced soil wall. *Transportation Research Record*, No. 1288, 109–116.

Bathurst, R. J. & Simac, M. R. (1994). Geosynthetic reinforced segmental retaining wall structures in North America. *Proceedings of the 5th International Conference on Geotextiles, Geomembranes and Related Products*, Singapore, 1275–1298.

Bathurst, R. J., Wawrychuk, W. F. & Jarrett, P. M. (1988). Laboratory investigation of two large-scale geogrid reinforced soil walls. *The Application of Polymeric Reinforcement in Soil Retaining Structures*, Jarrett, P. M. and McGown, A., Editors, Kluwer Academic Publishers, Dordrecht, pp. 71–125.

Bathurst, R. J., Benjamin, D. J. & Jarrett, P. M. (1989). An instrumented geogrid reinforced soil wall. *Proceedings of the Twelfth International Conference on Soil Mechanics and Foundation Engineering*, Rio de Janeiro, **2**, 1223–1226.

Bathurst, Jarrett & Associates Inc. (1996a). *Report on Results of Pisa II Block Unit Interface Shear Capacity Testing*. Bathurst, Jarrett & Associates Inc., Kingston, Ontario.

Bathurst, Jarrett & Associates Inc. (1996b). *Report on Results of Pisa II Unit with Stratagrid 200 Connection Capacity Testing. Bathurst, Jarrett & Associates Inc.,* Kingston, Ontario.

Bell, J. R., Barrett, R. K. & Ruckman, A. C. (1983). Geotextile earth-reinforced retaining wall tests: Glenwood Canyon, Colorado. *Transportation Research Record*, No. 916, 59–69.

Berg, R.R., Bonaparte, R., Anderson, R. P. & Chouery, V. E. (1986). Design, construction and performance of two geogrid reinforced soil retaining walls. *Proceedings of the 3rd International Conference on Geotextiles*, Vienna, 401–406.

Bergado, D. T., Shivashankar, R., Sampaco, C. L., Alfaro, M. C. & Anderson, L. R. (1991). Behaviour of a welded wire wall with poor quality, cohesive-friction backfill on soft Bangkok clay: a case study. *Canadian Geotechnical Journal*, **28**, 860–880.

Bergado, M. T., Menil, N. J. L., Rimoldi, R. & Douglas, R. S. (1994). Performance of full scale embankment on soft Bangkok clay with geogrid reinforcement. *Proceedings of the 5th International Conference on Geotextiles, Geomembranes and Related Products*, Singapore, 1–4.

Biot, M. A. (1941). General theory of three-dimensional consolidation. *Journal of Applied Physics*, **12**, 155–164.

Bjerrum, L. (1973). Problems of soil mechanics and construction on soft and structurally unstable soils (collapsible, expansive and others). *Proceedings of the 8th International Conference on Soil Mechanics and Foundation Engineering*, Moscow, **3**, 111–159.

Bloomfield, R. A., Soliman, A. F. & Abraham, A. (2001). Performance of mechanically stabilized earth walls over compressible soils. In *Landmarks in Earth Reinforcement*, Ochiai, H. and Yasufuku, N. (eds), Swets and Zeitlinger, Balkema, pp. 317–322.

Bolton, M. D. (1986). The strength and dilatancy of sands. *Géotechnique*, **36**, No. 1, 65–78.

Canadian Geotechnical Society (CGS) (1992). *Canadian Foundation Engineering Manual*, 3rd edn, CGS, Richmond, British Columbia.

Carter, J. P. & Balaam, N. P. (1990). *Program AFENA: A General Finite Element Algorithm*. Centre for Geotechnical Research, University of Sydney, New South Wales.

Chen, W. F. & Mizuno, E. (1990). *Non-Linear Analysis in Soil Mechanics: Theory and Implementation*, Developments in Geotechnical Engineering 53, Elsevier, New York.

Chou, N. N. S. & Wu, J. T. H. (1993). Effects of foundation on the performance of geosynthetic-reinforced soil walls. *Proceedings of Geosynthetics 1993*, Vancouver, **1**, pp. 189–202.

Craig, R. F. (1992). *Soil Mechanics*, 5th edn, Chapman & Hall, New York.

Curtis, R. L., Chouery-Curtis, V. E. & Miller, D. A. (1988). Geogrid reinforced soil wall on compressible soils. *Proceedings of the 2nd International Conference on Case Histories in Geotechnical Engineering*, St Louis, 1063–1067.

Davis, E. H. & Booker, J. R. (1973). The effect of increasing strength with depth on the bearing capacity of clays. *Géotechnique*, **23**, No. 4, 551–563.

Davis, E. H. & Poulos, H. G. (1968). The use of elastic theory for settlement prediction under three-dimensional conditions. *Géotechnique*, **18**, 67–91.

Dittrich, J. P. (2000). *Slope Behaviour During Excavation of the Sarnia Approach to the St Clair Tunnel*. PhD thesis, Faculty of Engineering Science, University of Western Ontario.

Duncan, J. M., Byrne, P., Wong, K. S. & Mabry, P. (1980). *Strength, Stress–Strain and Bulk Modulus Parameters for Finite Element Analysis of Stresses and Movement in Soil Masses*, Geotechnical Engineering Report No. UCB/GT/80–01, University of California, Berkeley.

Federal Highway Administration (FHWA) (1996). *Mechanically Stabilized Earth Walls and Reinforced Soil Slopes, Design and Construction Guidelines*, FHWA Demonstration Project 82, Publication Number FHWA-SA-96-071.

Gnanendran, C. T. (1993). *Observed and Calculated Behaviour of a Geotextile Reinforced Embankment on a Soft Compressible Soil*. PhD thesis, Faculty of Engineering Science, University of Western Ontario.

GRI Standard and Practice (1991). *GG-4 (a & b): Determination of Long-Term Design Strength of (Stiff and Flexible) Geogrids*, Geosynthetic Research Institute, Drexel University, Philadelphia, PA.

Helwany, S. M. B., Reardon, G. & Wu, J. T. H. (1999). Effects of backfill on the performance of GRS retaining walls. *Geotextiles and Geomembranes*, **17**, No. 1, 1–16.

Ho, S. K. P. & Rowe, R. K. (1993). Finite element analysis of geosynthetic-reinforced soil walls. *Proceedings of Geosynthetics '93*, Vancouver, pp. 203–216.

Holtz, R. D. & Kovacs, W. D. (1981). *An Introduction to Geotechnical Engineering*, Prentice Hall, Englewood Cliffs.

Industrial Fabrics Association International (IFAI) (1999). *2000 Specifier's Guide*, GFR, **17**, No. 9, Industrial Fabrics Association International, Roseville, MN.

Janbu, N. (1963). Soil compressibility as determined by oedometer and triaxial tests. *Proceedings of the European Conference on Soil Mechanics and Foundation Engineering*, Wiesbaden, pp. 19–25.

Karpurapu, K. & Bathurst, R. J. (1992). Analysis of geosynthetic reinforced soil wall by the finite element method. *Proceedings of the 4th International Conference on Numerical Models in Geomechanics: NUMOG 4*, Swansea, 861–870.

Kirschner, R. & Hermansen, E. (1994) Abutments in reinforced soil for a road bridge. *Proceedings of the 5th International Conference on Geotextiles, Geomembranes and Related Products*, Singapore, 259–260.

Koerner, R. K. (1990). *Designing with Geosynthetics*, 4th edn, Prentice Hall, Englewood Cliffs, NJ.

Kojima, K., Tateyama, M., Sakamoto, N. & Maruyama, O. (1996). Geosynthetic-reinforced soil retaining wall using clay on a very soft ground for Hokuriku bullet train yard in Nagano. *Earth Reinforcement*, Ochiai, H., Yasufuku, N. and Omine, K., Editors, Balkema, Rotterdam/Brookfield, pp. 227–232.

Krieger, J., Erban, P. J. & Thamm, B. R. (1994). Numerical analysis of full-scale tests on geosynthetic reinforced retaining walls. *International Journal of Computer Application in Technology*, **7**, No. 3–6, 242–250.

Kulhawy, F. H. & Mayne, P. W. (1990). *Manual on Estimating Soil Properties for Foundation Design*, Research Project 1493-6, Cornell University, New York.

Kumada, T., Otani, Y. & Matsui, T. (1992). Practice and design of reinforced-earth bridge abutments on soft ground. *Earth Reinforcement Practice*, Ochiai, H., Hayashi, S. and Otani, J., Editors, Balkema, Rotterdam/Brookfield, pp. 373–378.

Li, A. L. (2000). *Time Dependent Behaviour of Reinforced Embankments on Soft Foundations*. PhD thesis, Faculty of Engineering Science, University of Western Ontario.

Li, A. L. & Rowe, R. K. (1999). Reinforced embankments over soft foundations under undrained and partially drained conditions. *Geotextiles and Geomembranes*, **17**, No. 3, 129–146.

Mesri, G., Lo, D. O. K. & Feng, T. W. (1994). Settlement of embankments on soft clays, Keynote Lecture. *Settlement '94*, Texas A&M University, Geotechnical Special Publication 40, ASCE, Reston, **1**, pp. 8–56.

Michalowski, R. L. (1998). Limit analysis in stability calculations of reinforced soil structures. *Geotextiles and Geomembranes*, **16**, No. 6, 311–331.

Nakajima, T., Toriumi, N., Shintani, H., Miyataka, H. & Dobahi, K. (1996). Field performance of a geotextile reinforced soil wall with concrete facing blocks. *Earth Reinforcement*, Ochiai, H., Yasufuku, N. and Omine, K., Editors, Balkema, Rotterdam/Brookfield, pp. 427–432.

National Concrete Masonry Association (NCMA) (1996). *Design Manual for Segmental Retaining Walls*, 2nd edn, NCMA, Herndon, VA.

Ochiai, Y. & Fukuda, N. (1996). Experimental study on geotextile-reinforced soil walls with different facing. *Symposium on Geosynthetics: Application, Design and Construction*, de Groot, M. B., den

Hoedt, G. and Termaat, R. J., Editors, Balkema, Rotterdam/Brookfield, pp. 113–120.
Otani, J., Hirai, T., Ochiai, H. & Shinowaki, S. (1998). Evaluation of foundation support for geosynthetic reinforced soil wall on sloping ground. *Proceedings of the 6th International Conference on Geosynthetics*, Atlanta, 601–603.
Palmeira, E. M. & Monte, L. M. (1997). The behaviour of model reinforced walls on soft soils. *Proceedings of Geosynthetics '97*, Long Beach, California, 73–84.
Perzyna, P. (1963). The constitutive equations for work-hardening and rate sensitive plastic materials. *Proceedings of Vibration Problems*, Warsaw, **4**, No. 3, 281–290.
Porbaha, A., Zhao, A., Kobayashi, M. & Tishida, T. (2000). Upper bound estimate of scaled reinforced retaining walls. *Geotextiles and Geomembranes*, **18**, No. 6, 403–413.
Poulos, H. G. & Davis, E. H. (1974). *Elastic Solutions for Soil and Rock Mechanics*, Wiley, New York.
Rowe, R. K. (2000). *Geotechnical Design using Geosynthetics*, ES707 Course Notes. University of Western Ontario, London, Ontario.
Rowe, R. K. & Hinchberger, S. D. (1998). The significance of rate effects in modelling the Sackville test embankment. *Canadian Geotechnical Journal*, **35**, No. 3, 500–516.
Rowe, R. K. & Ho, S. K. P. (1993). A review of the behaviour of reinforced soil walls. *Earth Reinforcement*, Ochiai, H., Hayashi, S. and Otani, J., Editors, Balkema, Rotterdam/Brookfield, pp. 801–830.
Rowe, R. K. & Ho, S. K. P. (1996). Some insights into reinforced wall behaviour based on finite element analysis. *Earth Reinforcement*, Ochiai, H., Yasufuku, N. and Omine, K., Editors, Balkema, Rotterdam/Brookfield, pp. 485–490.
Rowe, R. K. & Skinner, G. D. (2001). Numerical analysis of geosynthetic reinforced retaining wall constructed on a layered soil foundation. *Geotextiles and Geomembranes*, **19**, 387–412.
Rowe, R. K. & Soderman, K. L. (1987). Stabilization of very soft soils using high strength geosynthetics: the role of finite element analysis. *Geotextiles and Geomembranes*, **6**, No. 1-3, 53–80.
Schlosser, F. & Guilloux, A. (1982). Reinforced Earth uses on soft soils. *Proceedings of the International Symposium on Recent Developments in Ground Improvement Techniques*, Bangkok, Balasubramanian, A. S., Chandra, S. and Bergado, D. T., Editors, pp. 145–152.
Schmertmann, G. R., Chew, S. H. & Mitchell, J. K. (1989). *Finite Element Modelling of Reinforced Soil Wall Behaviour*, Department of Civil Engineering, University of California, Berkeley, Geotechnical Engineering Report No. UCB/GT/89-01.
Skinner, G. D. (2002). *Geosynthetic Reinforced Soil Walls Constructed on Yielding Foundations*, PhD thesis, Faculty of Applied Science, Queen's University, Kingston, Ontario.
Slope/W (2001). *Slope/W for Slope Stability Analysis*, Geo-slope International Ltd, Calgary, Alberta.
Tavenas, F., Jean, P., Leblond, P. & Leroueil, S. (1983). The permeability of natural soft clays. Part II: Permeability characteristics. *Canadian Geotechnical Journal*, **20**, No. 4, pp. 645–660.
Terzaghi, K., Peck, R. B. & Mesri, G. (1996). *Soil Mechanics in Engineering Practice*, 3rd edn, Wiley, New York.
Tsukada, Y., Ochiai, Y., Miyataka, H. & Tajiri, T. (1998). Field performance of a geosynthetic-reinforced soil wall with rigid facing. *Proceedings of the 6th International Conference on Geosynthetics*, Atlanta, 577–580.
Wu, J. T. H. (1992a). Measured behaviour of the Denver walls. *Proceedings of the International Symposium on Geosynthetic-Reinforced Soil Walls*, Denver, Balkema, Rotterdam/Brookfield, pp. 31–42.
Wu, J. T. H. (1992b). Predicting performance of the Denver walls: general report. *Proceedings of the International Symposium on Geosynthetic-Reinforced Soil Walls*, Denver, Balkema, Rotterdam/Brookfield, pp. 3–20.
Yoo, C. & Kim, J.-S. (2001). Effects of foundation stiffness and surface loading on the behaviour of soil-reinforced segmental retaining walls. *Proceedings of Geosynthetic Conference 2001*, Portland, OR, pp. 373–385.

The Editors welcome discussion in all papers published in Geosynthetics International. Please email your contribution to discussion@geosynthetics-international.com by 15 August 2004.